Cancer Research

Cyclin E Associates with the Lipogenic Enzyme ATP-Citrate Lyase to Enable Malignant Growth of Breast Cancer Cells

Kimberly S. Lucenay[1], Iman Doostan[1], Cansu Karakas[1], Tuyen Bui[1], Zhiyong Ding[2], Gordon B. Mills[2], Kelly K. Hunt[3], and Khandan Keyomarsi[1]

Abstract

Cyclin E is altered in nearly a third of invasive breast cancers where it is a powerful independent predictor of survival in women with stage I–III disease. Full-length cyclin E is posttranslationally cleaved into low molecular weight (LMW-E) isoforms, which are tumor-specific and accumulate in the cytoplasm because they lack a nuclear localization sequence. We hypothesized that aberrant localization of cytosolic LMW-E isoforms alters target binding and activation ultimately contributing to LMW-E–induced tumorigenicity. To address this hypothesis, we used a retrovirus-based protein complementation assay to find LMW-E binding proteins in breast cancer, identifying ATP-citrate lyase (ACLY), an enzyme in the *de novo* lipogenesis pathway, as a novel LMW-E–interacting protein in the cytoplasm. LMW-E upregulated ACLY enzymatic activity, subsequently increasing lipid droplet formation, thereby providing cells with essential building blocks to support growth. ACLY was also required for LMW-E–mediated transformation, migration, and invasion of breast cancer cells *in vitro* along with tumor growth *in vivo*. In clinical specimens of breast cancer, the absence of LMW-E and low expression of adipophilin (PLIN2), a marker of lipid droplet formation, associated with favorable prognosis, whereas overexpression of both proteins correlated with a markedly worse prognosis. Taken together, our findings establish a novel relationship between LMW-E isoforms of cyclin E and aberrant lipid metabolism pathways in breast cancer tumorigenesis, warranting further investigation in additional malignancies exhibiting their expression. *Cancer Res; 76(8); 2406–18. ©2016 AACR.*

Introduction

Our knowledge of inherited abnormalities leading to breast cancer have advanced significantly in recent years; however, an understanding of how the molecular events that are found in sporadic breast cancer integrate to regulate tumor initiation and progression has remained largely elusive for this complex disease. Cancer cells often exhibit uncontrolled proliferation due to deregulation of the cell cycle and of members of the cell-cycle regulatory pathways. Deregulation of cyclin E results from gene amplification, protein overexpression, and posttranslational cleavage in multiple tumor types leading to genomic instability and centrosome amplification (1). Moreover, cyclin E has shown to be an independent predictor of survival in patients with invasive breast cancer (2).

Full-length cyclin E protein (EL; 50 kDa) is posttranslationally cleaved by elastase into two low molecular weight (LMW) isoforms, LMW-E (T1; 45 kDa) and LMW-E (T2; 33 kDa; ref. 3). The significance of these tumor-specific LMW-Es, which was originally discovered in breast cancer by our group and subsequently by others (4–6), has recently been the subject of several review articles (7–9). These isoforms are also found in ovarian cancer (10, 11), melanoma (12), colorectal cancer (13–16), lung cancer (17), and renal cell carcinoma (18). Transgenic mice expressing the LMW-E isoforms have increased mammary tumor development and metastasis compared with mice-expressing EL (19). In addition, the LMW-E isoforms have greater affinity toward cyclin-dependent kinase 2 (CDK2) and are less sensitive to inhibition by the CDK inhibitors p21 and p27 (20, 21). Significantly, the LMW-E isoforms lack a classical nuclear localization sequence that targets cyclin E to the nucleus and thus preferentially accumulate in the cytoplasm (22, 23). Together, these data suggest that the biologic and chemical differences between EL and LMW-E isoforms are due to disparate protein interactions in the cytoplasm. Therefore, we hypothesized that aberrant localization of LMW-E isoforms in the cytoplasm leads to binding interactions and altered activation of cytoplasmic proteins that ultimately contribute to LMW-E tumorigenicity.

To further understand the role of the LMW-E isoforms in breast cancer tumorigenesis, we used a retrovirus-based protein complementation assay (RePCA) to identify LMW-E (T1) protein interactions in the cytoplasm. RePCA was first developed to identify AKT1-binding partners and is an effective system for discovering novel protein–protein interactions in an endogenous environment (24). Using this methodology, we identified ATP-citrate lyase (ACLY) as a novel interacting protein of

[1]Department of Experimental Radiation Oncology, The University of Texas MD Anderson Cancer Center, Houston, Texas. [2]Department of Systems Biology, The University of Texas MD Anderson Cancer Center, Houston, Texas. [3]Department of Breast Surgical Oncology, The University of Texas MD Anderson Cancer Center, Houston, Texas.

Note: Supplementary data for this article are available at Cancer Research Online (http://cancerres.aacrjournals.org/).

Corresponding Author: Khandan Keyomarsi, Department of Experimental Radiation Oncology, The University of Texas MD Anderson Cancer Center, 6565 MD Anderson Blvd, Box 1052, Houston, TX 77030. Phone: 713-792-4845; Fax: 713-794-5369; E-mail: kkeyomar@mdanderson.org

doi: 10.1158/0008-5472.CAN-15-1646

LMW-E (T1) in the cytoplasm. ACLY catalyzes the first step of the *de novo* lipogenesis pathway and converts cytoplasmic citrate to acetyl-CoA and oxaloacetate. We found that LMW-E upregulates ACLY enzymatic activity and subsequent lipid production in human mammary epithelial cells. Moreover, ACLY is required for LMW-E–mediated transformation *in vitro* and tumorigenesis *in vivo*. Finally, lack of LMW-E and low adipophilin (a marker for lipid droplet formation in human tissue) in 100 breast cancer specimens were associated with a favorable prognosis, whereas overexpression of both proteins was correlated with a significantly worse prognosis. Our data implicate a novel link between metabolic pathways and the deregulated cell cycle in breast cancer.

Materials and Methods

Cell culture and plasmids

MCF7 and MCF7 Tet-On cells were purchased from BD Clontech and cultured as described previously (25). The LMW-E (T1) intensely fluorescent protein N-terminus (IFPN) construct was generated previously (23) and used to create MCF7 Tet-On cells stably expressing the LMW-E (T1)-IFPN construct by selection with 80 μg/mL zeocin (Invitrogen). Embryonic kidney HEK 293T/17 cells from ATCC were cultured in DMEM supplemented with 10% FBS. RePCA plasmids IC1, IC2, and IC3 and packaging plasmids pcGP and pVSVG were used to produce the RePCA retrovirus. The immortalized nontumorigenic human mammary epithelial cell line, 76NE6, which ectopically expresses cyclin E isoforms under a doxycycline-inducible promoter, was cultured as described previously (26). 76NE6 tumor-derived cells (TDC) were cultured as described previously (26). Short hairpin (shRNA) constructs were purchased from the shRNA and ORFeome core at the University of Texas MD Anderson Cancer Center (Houston, TX) and were generated in a lentiviral packaging system as described previously (27). All cells were free of mycoplasma contamination. Cell lines were identified and authenticated by karyotype and short tandem repeat analysis using the MD Anderson's Characterized Cell Line Core Facility regularly (every 6 months).

RePCA

RePCA was performed as described previously (24). Briefly, IC1, IC2, or IC3 retrovirus were produced in HEK 293T/17 cells and subsequently used to transduce 1×10^7 MCF7 Tet-On cells stably expressing the LMW-E (T1)–IFPN construct. MCF7 cells display very low endogenous levels of LMW-E that will not compete with the tagged overexpressed forms. Puromycin-resistant cells were subjected to fluorescence-activated cell sorting for GFP expression using a BD FACSAria II cell sorter (BD Biosciences). Single cells were grown at low density in minimal essential medium-α containing 2 μg/mL puromycin to form clones. The clones were expanded and RNA was extracted using RNAeasy mini kits (Qiagen). Reverse transcription was performed with a random primer (RT-1) as described previously (24). The cDNA was amplified by PCR with an intensely fluorescent protein C-terminus (IFPC)-specific primer and a T7 primer (24) using HotStarTaq DNA polymerase (Qiagen). PCR products were gel purified and sequenced at the Sequencing and Microarray Facility at the MD Anderson Cancer Center. Sequences were identified using GenBank BLAST (24).

Immunocytochemical analysis and lipid staining

RePCA clones were cultured in the presence of 2 μg/mL doxycycline for 48 hours. Cells were fixed with 4% paraformaldehyde, and nuclei were counterstained with 4,6-diamidino-2-phenylindole (DAPI; Sigma-Aldrich). Lipid staining was conducted using the LipidTox reagent according to the manufacturer's instructions (Invitrogen). LipidTox reagent was diluted and incubated with cells for 45 to 60 minutes. Images were captured on an Olympus Epi-fluorescence microscope and Hamamatsu Orca camera.

ACLY activity

ACLY activity was measured by the malate dehydrogenase–coupled method as described previously (28). This method can be used with either pure enzyme or crude cell lysates (28–30), as we have used in this study. Briefly, cell lysates were extracted from MCF7 and 76NE6 cell lines and incubated with the reaction mixture (200 mmol/L Tris HCl pH 8.7, 20 mmol/L $MgCl_2$, 20 mmol/L potassium citrate, 1 mmol/L DTT, 0.2 mmol/L NADH, 1 U/mL MDH, 0.5 mmol/L CoA) with and without ATP. ACLY activity was measured every 3 minutes for 30 minutes using a NanoDrop 2000c spectrophotometer from Thermo Fisher Scientific. ACLY-specific activity was calculated as the change in absorbance with ATP minus the change in absorbance without ATP normalized to protein concentration. *In vitro* assays used 25 ng of purified recombinant ACLY enzyme (United States Biological).

In vivo xenograft model

Nude mice were obtained from the Department of Experimental Radiation Oncology at The University of Texas MD Anderson Cancer Center. MCF7 cells were injected in a 50:50 ratio of cells: Matrigel at a density of 2.5×10^6 cells/100 μl into inguinal mammary fat pads bilaterally (No. 5 and 10). Tumors were measured twice per week with caliper starting at 3 weeks for 12 weeks. Maximum tumor volume per mouse reached 1,500 mm^3. The Institutional Animal Care and Use Committee (IACUC) protocol for this study, #00001188-RN01 entitled "Gene Therapy Approaches to Solid Tumors Using Tumor Suppressor Genes," was approved by The IACUC at The University of Texas MD Anderson Cancer Center (Houston, TX).

Breast cancer patients

We utilized a patient cohort of 100 stage I–III breast cancer patients enrolled in a study between January 2000 and June 2010 (Lab00-222); the study was approved by MD Anderson's Institutional Review Board. Formalin-fixed, paraffin-embedded tissue and clinical and pathologic information were collected from all patients. Patients were also followed for recurrence and survival. Clinical characteristics of the patients are listed in Supplementary Table S1.

Oil Red O and immunohistochemical staining

Frozen sectioned tissue slides were air dried and fixed with 4% paraformaldehyde and stained with Oil Red O solution (0.5 g Oil Red O in 100 mL propylene glycol) for 30 minutes at room temperature and rinsed under running tap water for 10 minutes. Slides were lightly stained with alum hematoxylin for 1 minute, rinsed with distilled water, and mounted for microscopy. Immunohistochemistical staining on formalin-fixed paraffin-embedded tissues was performed using cyclin

E, ACLY, Ki-67 and adipophilin antibodies in tumor tissue samples from mouse xenografts and breast cancer patients. The immunohistochemical staining protocol and scoring system used for each antibody is described in detail in Supplementary Methods.

Statistical analysis

All experiments were performed at least in triplicates with at least three technical replicates per experiment if not otherwise indicated. The results of each experiment are reported as the mean of experimental replicates. Error bars represent the SD from the mean. If not otherwise indicated, pairwise comparisons were analyzed using the unpaired two-sided *t* test (GraphPad Prism). For all tests, $P<0.05$ was considered significant.

Results

Interacting partners of LMW-E (T1) identified in RePCA screen

To identify LMW-E (T1) binding proteins in the cytoplasm, we utilized RePCA system (24). Tet-On MCF7 cells stably expressing the LMW-E (T1) isoforms were transduced with the RePCA retrovirus. Following infection, 80,000 fluorescent cells gave rise to 204 colonies and 29.9% (61/204) retained fluorescence following doxycycline induction. From the 61 colonies, we identified 11 independent LMW-E (T1) interacting proteins (Supplementary Table S2). Sequencing the individual clones revealed the IFPC fusion transcript integrated at or near the transcriptional start site in 6 of 11 transcripts, indicating full-length or near-full-length proteins were generated. We found the majority of the interacting proteins identified (8/11, 73%) displayed known localization to the cytoplasm. For example, YWHAQ (14-3-3β) regulates protein signaling by binding phosphoserine-containing proteins (31). HSP27 is a chaperone protein induced upon environmental stress (32). VAMP8 (vesicle-associated membrane protein 8) is a component of a protein complex involved in the docking of synaptic vesicles with the presynaptic membrane (33). RPL41 (ribosomal protein L41) is a component of the 60S subunit of the ribosome and important for mitosis and centrosome integrity. RANBP1 is a GTPase that facilitates protein transport across the nuclear membrane (34). The largest functional group (3/11, 27%) of proteins discovered from the screen were proteins involved in metabolism. *Trans*-2,3-Enoyl-CoA reductase (TECR) catalyzes the final step in synthesizing long and very long-chain fatty acids (35). Aldolase A (ALDO-A), also known as fructose bisphosphate aldolase, plays a key role in glycolysis and gluconeogenesis (36). Finally, ACLY, catalyzes the first step of the *de novo* lipogenesis pathway and converts cytoplasmic citrate to acetyl-CoA and oxaloacetate (37). Elevated ACLY protein and activity levels have been shown to correlate with tumor growth and progression in breast carcinoma, lung adenocarcinoma, and glioblastoma (28, 36, 38), whereas ACLY inhibition by genetic or pharmacologic methods suppresses tumor growth (29). On the basis of its role in promoting tumor growth and its novel interaction with cyclin E, we selected ACLY for further investigation.

Cyclin E and ACLY are interacting proteins

To examine the localization of the LMW-E (T1) protein complexes, we subjected several RePCA clones to fluorescence microscopy. The LMW-E (T1)/ACLY interaction was identified in clones #18 and #46 (Fig. 1A) and as expected, the complex was localized primarily to the cytoplasm. Another clone, #16 (used as a control), identified an interaction between LMW-E (T1) and VAMP8, and this interaction was localized to the plasma membrane. The LMW-E (T1)/ACLY interaction was further validated by coimmunoprecipitation from cells coexpressing myc-ACLY and either EL or T1 N-terminally tagged with SFB (S-tag, Flag epitope tag, and streptavidin-binding peptide tag; Fig. 1B) or endogenously using three different breast cancer cell lines (MCF-7, MDA-MB-436, and MDA-MB-157; Supplementary Fig. S1). Because Cdk2 is the primary binding partner of cyclin E, we examined whether cyclin E or Cdk2 directly binds ACLY. A GST pull-down assay revealed cyclin E as the direct binding partner of ACLY (Fig. 1C) and further demonstrated that Cdk2 does not bind directly to ACLY. ACLY is phosphorylated posttranslationally by multiple proteins, including cAMP-dependent protein kinase, GSK3β, nucleoside diphosphate kinase (NDPK), and protein kinase B (Akt; refs. 39–41). Therefore, we examined whether ACLY is a substrate of the cyclin E/Cdk2 complex. An *in vitro* kinase assay revealed ACLY (aa 420-486) is not a substrate of EL/Cdk2 or T1/Cdk2 (Fig. 1D). Akt1, which phosphorylates ACLY at Ser454, was used as a positive control (28). Together, these results indicate that ACLY directly binds cyclin E without posttranslational modification.

LMW-E isoforms enhance ACLY enzymatic activity

ACLY enzymatic activity has shown to be elevated in breast carcinoma and lung adenocarcinoma compared with normal tissue (28, 36). Therefore, the effect of cyclin E expression on ACLY enzymatic activity was examined in human breast cancer, MCF7, cells ectopically expressing the cyclin E isoforms. Expression of LMW-E (T1) and LMW-E (T2) significantly increased ACLY enzymatic activity by 25% to 60%, whereas EL overexpression had no effect (Fig. 2A and B). We examined cyclin E expression on ACLY activity in another model system, in which the expression of FLAG-tagged vector, EL, LMW-E (T1), and LMW-E (T2) in 76NE6 cells could be induced by doxycycline (Fig. 2C and D). ACLY activity increases were only detected upon doxycycline induction of the LMW-E isoforms, but not EL (Fig. 2C). The phosphorylation of ACLY on Ser454 by Akt provides one mechanism for regulation of ACLY enzymatic activity, however, the increase in ACLY enzymatic activity observed upon expression of the LMW-E isoforms did not result in changes of total or phosphorylated ACLY protein levels in either model system, indicating the elevation in activity is independent of Akt (Fig. 2B and D; ref. 28). Finally, we examined the ability of different isoforms of cyclin E to increase enzymatic activity of purified ACLY in a cell free, *in vitro* assay. The results revealed that together LMW-E (T1) and LMW-E (T2) directly upregulate ACLY activity, and addition of EL or CDK2 did not result in significant elevation (Fig. 2E). Collectively, our findings suggest LMW-E (T1) and/or LMW-E (T2) isoforms activate ACLY compared in EL in all systems evaluated.

Cytoplasmic ACLY activation is associated with lipid accumulation

ACLY is primarily found in the cytoplasm, but also localizes to the nucleus in murine embryonic fibroblasts, murine pro-B-cell lymphoid cells, glioblastomas, and colorectal carcinomas (42). To examine whether the LMW-E isoforms specifically upregulate cytoplasmic ACLY activity, 76NE6 cells with inducible expression of cyclin E were fractionated (Fig. 3A) and assayed for ACLY activity (Fig. 3B). ACLY activity was higher in the cytoplasm

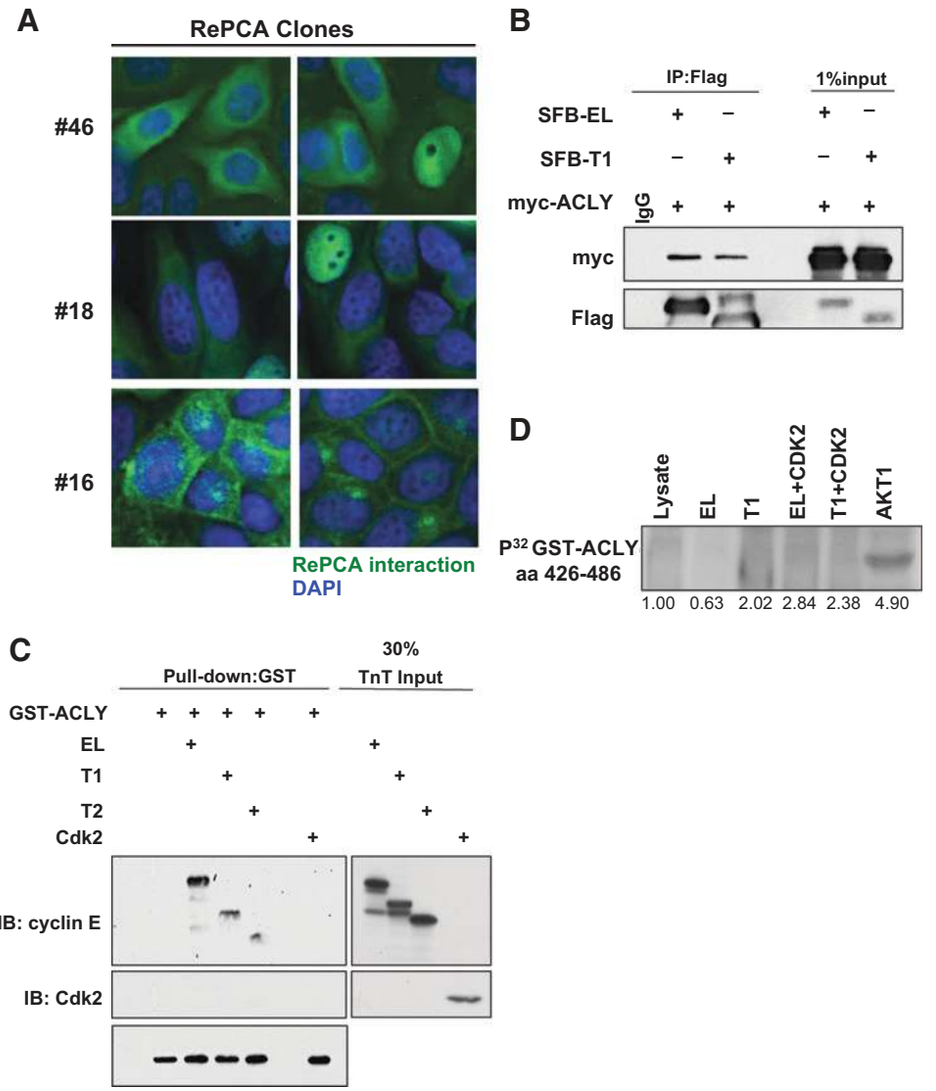

Figure 1.
Validation of RePCA clones. A, RePCA clone #46, #18, and #16 were fixed and counterstained with DAPI. B, 293T lysates expressing SFB-tagged cyclin E isoforms and myc-ACLY were immunoprecipitated using an anti-Flag antibody. C, recombinant GST-ACLY protein was incubated with *in vitro* transcribed and translated (TnT) cyclin E isoforms or Cdk2 and isolated using glutathione sepharose beads and subjected to Western blot analysis. D, *in vitro* kinase assay using recombinant GST-ACLY aa 426-486 and recombinant cyclin E isoforms produced in Sf9 cells alone or in complex with CDK2 were isolated by Cdk2 immunoprecipitation and incubated with GST-ACLY in the presence of ^{32}P-γ-ATP.

compared with the nucleus in all conditions examined, however, activity increased only in the cytoplasmic fraction of cells containing LMW-E compared with uninduced conditions (Fig. 3B). Importantly, induction of EL had no effect and nuclear LMW-E isoforms only increased ACLY activity by about 10% (Fig. 3B), suggesting that the cytoplasmic interaction between LMW-E and ACLY results in elevated ACLY activity.

End products of the *de novo* lipogenesis pathway include phospholipids and complex fatty acids, resulting in lipid droplet formation (43). Lipid droplets are intracellular structures comprised of a phospholipid and sterol outer layer and hydrophobic core containing neutral lipids such as triacylglycerides and cholesteryl esters (44). To measure lipid accumulation, cyclin E–inducible 76NE6 cells were stained with a neutral lipid dye. Lipid staining under uninduced conditions showed a diffuse pattern in all cells, however, doxycycline induction in LMW-E–expressing cells revealed a punctate staining pattern, indicating lipid droplet formation (Fig. 3C). Quantitation of the lipid droplet–containing cells showed a significant increase when LMW-E was induced (Fig. 3D). Next, to examine whether lipid droplet accumulation in LMW-E expressing cells requires ACLY, ACLY was downregulated in the LMW-E inducible cells (Fig. 3D and E). Results revealed that lipid droplets were present in only 20% to 30% of cells when ACLY was downregulated, compared with 40% to 60% in control shRNA, suggesting that expression of LMW-E (T2) is insufficient to induce lipid droplet formation in the absence of ACLY (Fig. 3G and H). Together, these data show that ACLY is highly active in the cytoplasm due to the presence of LMW-E and results in lipid droplet formation in human mammary epithelial cells.

ACLY is required for LMW-E–mediated transformation

To examine the requirement of ACLY in LMW-E–mediated transformation, we performed an anchorage-independent growth assay in MCF-7 overexpressing the cyclin E isoforms concomitantly with ACLY downregulation, which effectively reduced protein expression and enzymatic activity (Fig. 4A and B). ACLY downregulation had no effect on vector-expressing cells and only a slight reduction in anchorage-independent growth was observed in EL cells at 10 days (Fig. 4C, top), but was rescued by 30 days (Fig. 4C, bottom). However, ACLY downregulation in LMW-E–expressing

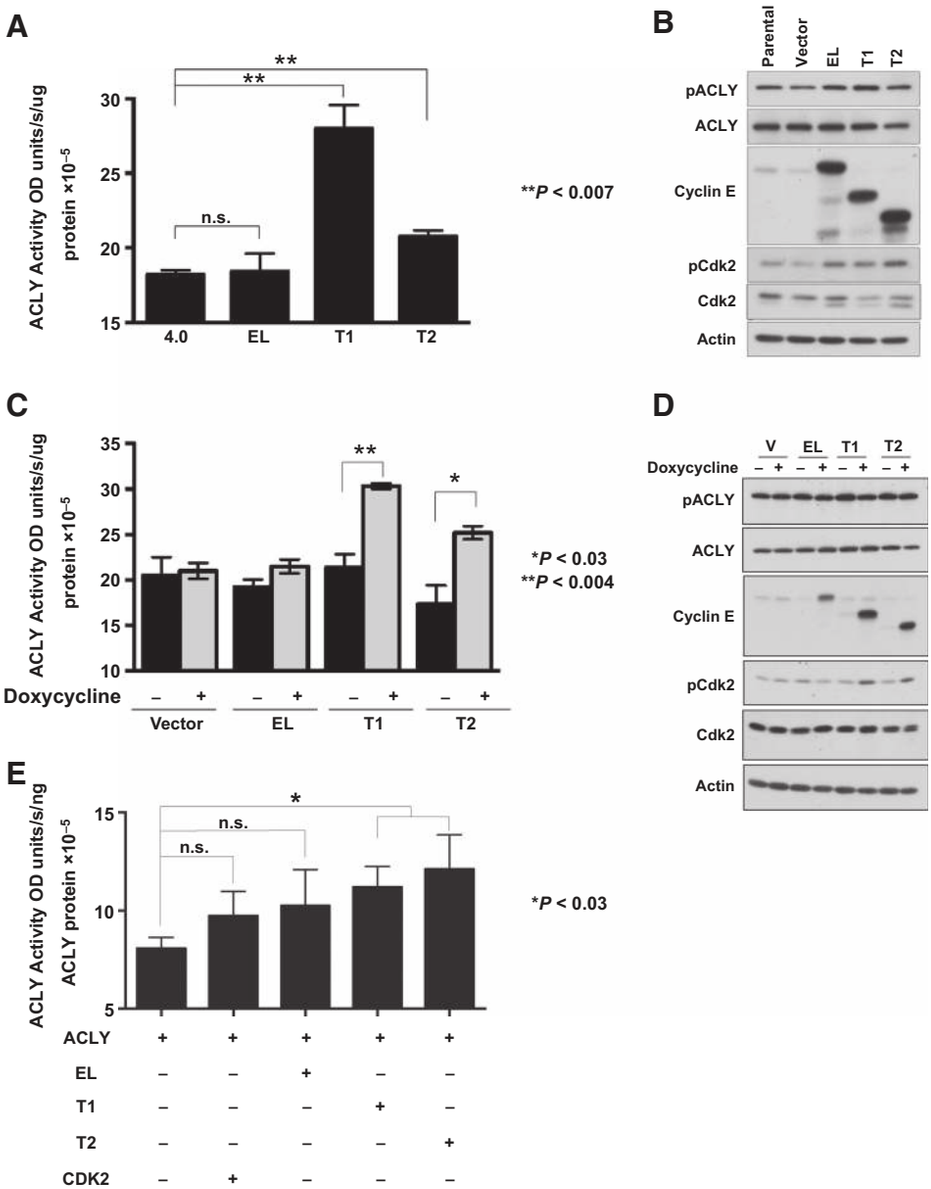

Figure 2.
LMW-E isoforms affect ACLY enzymatic activity. A, MCF7 cell lysates ectopically expressing the cyclin E isoforms were used to examine ACLY enzymatic activity by the malate dehydrogenase coupled method. Error bars, SEM from three independent replicates (Student *t* test; **, $P < 0.007$). B, Western blot analysis showing protein expression. C, 76NE6 lysates containing inducible expression of the LMW-E isoforms increases ACLY enzymatic activity. Error bars, SEM from three independent replicates (Student *t* test; *, $P < 0.03$ and **, $P < 0.004$). D, Western blot analysis showing protein expression. E, *in vitro* transcribed and translated cyclin E isoforms or CDK2 were incubated with purified ACLY protein and subjected to the malate dehydrogenase coupled method. Error bars, SEM from three independent replicates (Student *t* test; **, $P < 0.03$).

cells resulted in a significant reduction in colony formation at 10 days, which was not rescued by 30 days (Fig. 4C). Moreover, the average colony diameter was reduced in the LMW-E but not EL expressing cells containing ACLY knockdown (Fig. 4D). Importantly, ACLY knockdown did not affect CDK2-associated kinase activity, suggesting that CDK2 activity does not account for the reduced colony size in LMW-E–expressing cells containing ACLY downregulation (Fig. 4E). Together, these data suggest that ACLY contributes to LMW-E–mediated transformation in the context of anchorage-independent growth.

ACLY downregulation reduces migratory and invasive capabilities of human mammary epithelial cells

ACLY has been implicated in regulating migration in glioblastoma (38). Moreover, it has been shown that LMW-E expression in nontumorigenic human mammary epithelial cells (76NE6-HMECs) that have been serially passaged three generations through mice; called TDCs, have an increased propensity to invade using a transwell invasion assay (26). To examine whether ACLY is required for LMW-E–mediated migration and invasion in TDCs, ACLY was downregulated using shRNA in the three different TDCs (Supplementary Fig. S2A and S2B). Cyclin E levels in these clones were reported previously (26, 27). A wound-healing assay showed that migration of LMW-E TDCs was significantly inhibited 30% to 50% within 24 hours in the ACLY knockdown cells compared with scrambled shRNA, whereas ACLY downregulation had minimal effect in the migration of parental or EL-expressing cells (Fig. 5A and B). Importantly, reduced migration was not due to changes in the proliferative or apoptotic capacity of the ACLY knockdown cells, as no changes were observed in Annexin V or bromodeoxyuridine (BrdUrd) positive cells (Fig. 5C). In addition, no significant changes were observed in

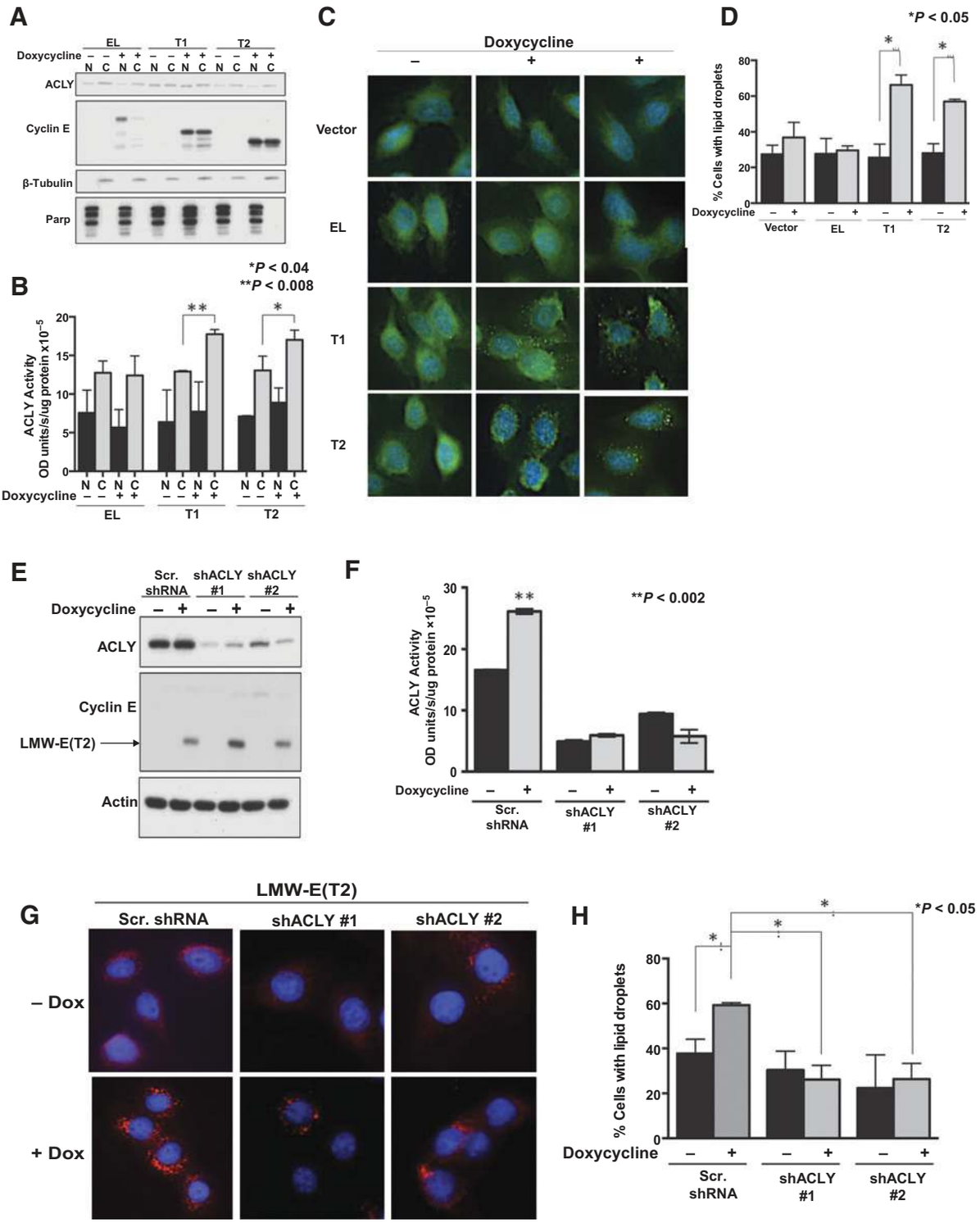

Figure 3.

Cytoplasmic ACLY activity results in lipid droplet accumulation. A, Western blot analysis showing protein expression from fractionated cells. N, nuclear fractions; C, cytoplasmic fraction. B, ACLY activity is shown for at least three independent replicates from fractionated 76NE6 cells using the malate dehydrogenase coupled method. Statistical analysis was conducted using the Student *t* test. Error bars, SEM (**, $P < 0.008$; *, $P < 0.04$). C, 76NE6 cell containing inducible expression of cyclin E stained with LipidTox and counterstained with DAPI. D, lipid droplet formation was quantified before and after addition of doxycycline ($n = 100$). Student *t* test; *, $P < 0.05$). E, Western blot analysis showing protein expression. F, 76NE6-inducible LMW-E(T2) lysates containing ACLY knockdown to examine ACLY activity. Three independent replicates are shown; error bars, SEM (**, $P < 0.002$). G, 76NE6- inducible LMW-E (T2) cells stained with LipidTox and counterstained with DAPI. H, cells were counted before and after addition of doxycycline ($n = 100$). (Student *t* test; *, $P < 0.05$).

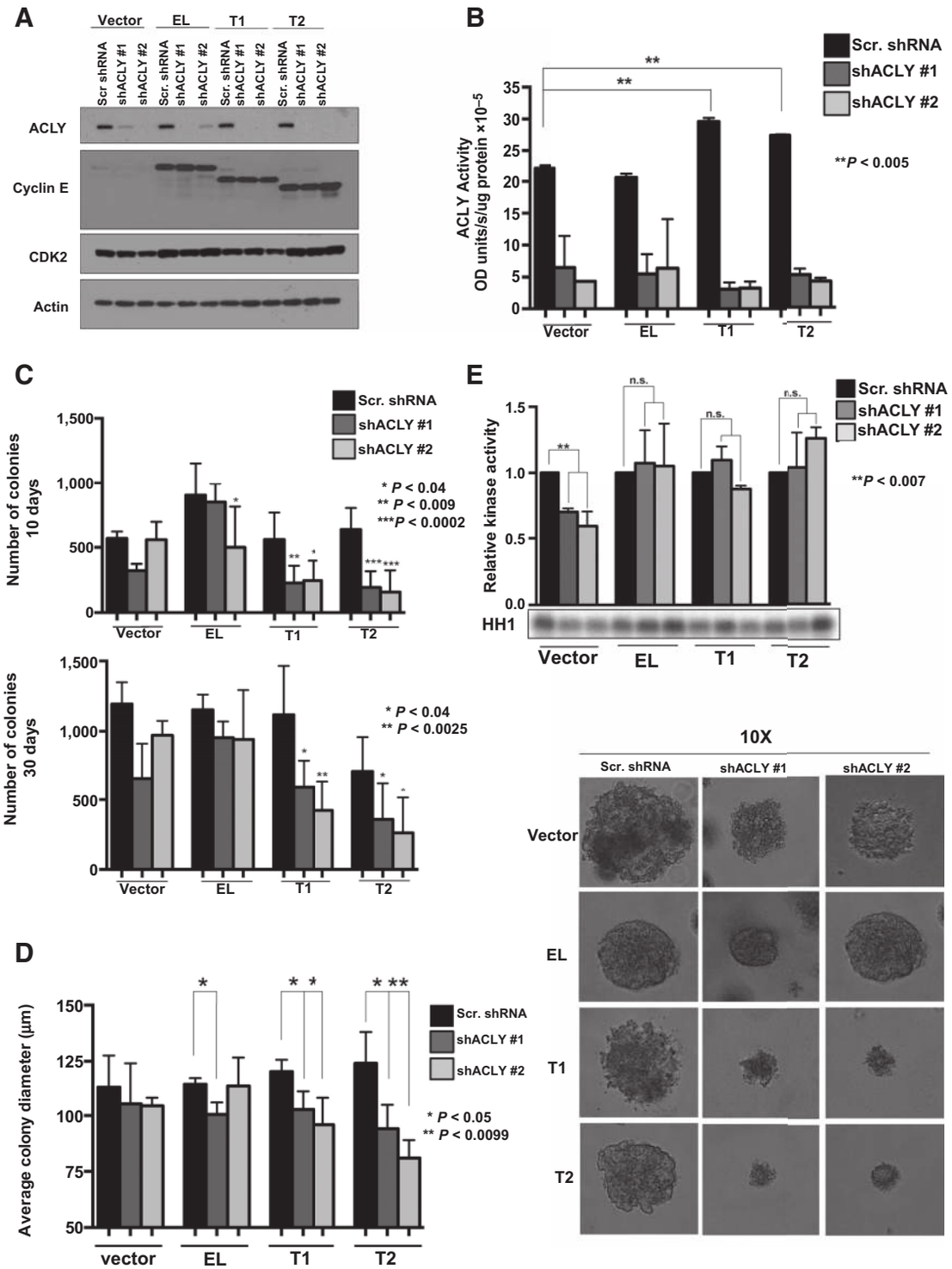

Figure 4.

ACLY is required for LMW-E–mediated anchorage-independent growth. A, Western blot analysis showing protein expression. B, MCF7 lysates ectopically expressing the cyclin E isoforms with ACLY downregulation were used to examine ACLY activity from two independent replicates. Error bars, SEM; **, $P < 0.005$. C, quantitation of colonies formed after 10 days and 30 days in anchorage-independent growth conditions of MCF7 cells ectopically expressing the cyclin E isoforms with ACLY downregulation. Statistical analysis was performed using the Student *t* test in three independent experiments performed in triplicate (10 days, $^{*}P < 0.04$, $^{**}P < 0.009$, $^{***}P < 0.0002$; 30 days, $^{*}P < 0.04$ and $^{**}P < 0.0025$). D, average colony diameter of colonies formed in soft-agar conditions. Statistical analysis was performed using the Student *t* test; (**, $P < 0.0085$) and performed in triplicate with images from representative colonies are shown. E, CDK2-associated kinase activity, using Histone H1 (HH1) as a substrate. n.s., not significant.

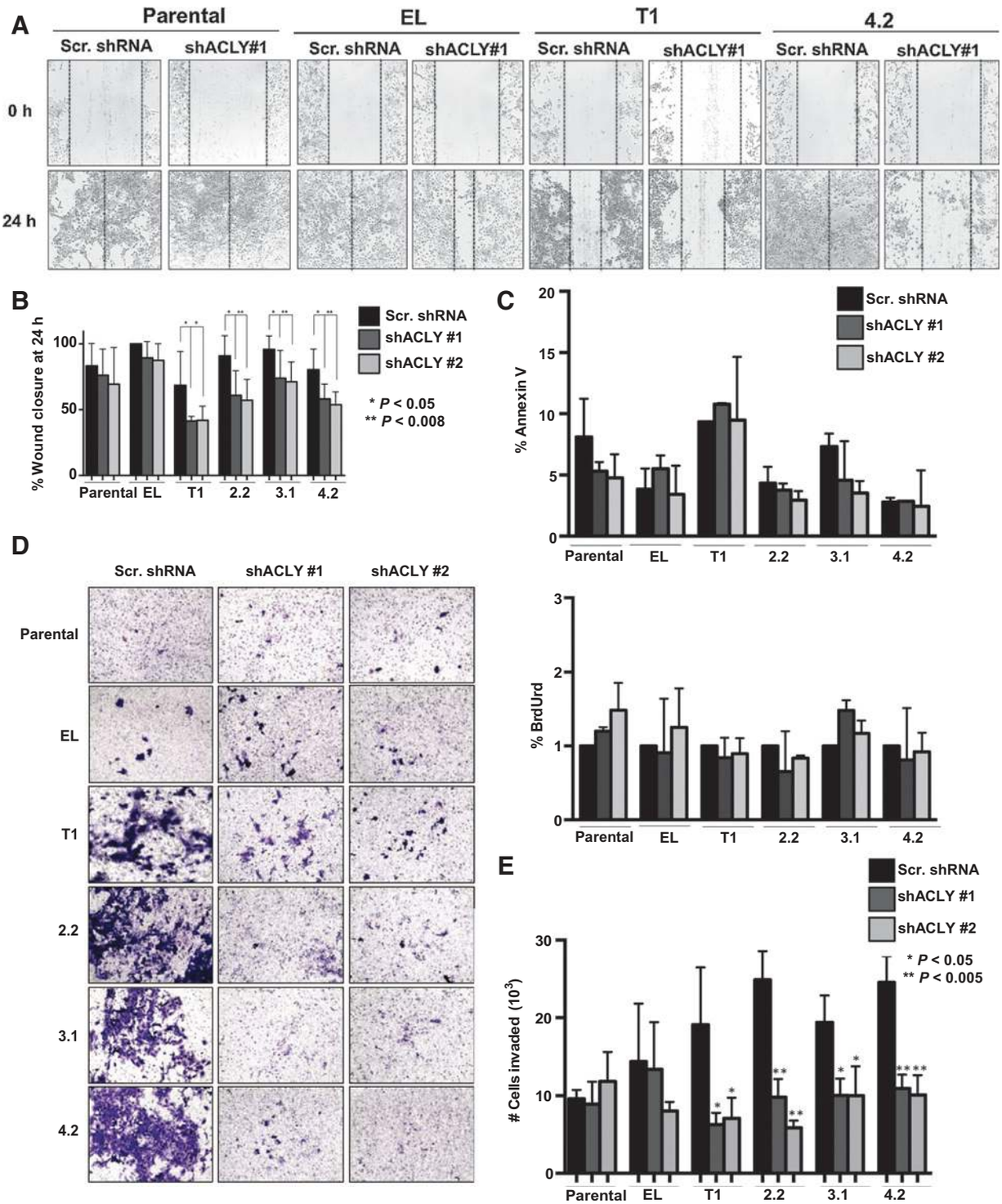

Figure 5.
Inhibition of ACLY reduces migration and invasion in HMECs. A, 76NE6 and TDCs containing either scrambled shRNA or shRNA toward ACLY reached confluency and scratched with a pipette tip to create a wound. Images were taken at 0 and 24 hours post-scratch. B, statistical analysis was conducted using the Student *t* test from three independent replicates. Error bars, SEM; *, $P < 0.05$ and **, $P < 0.008$. C, 76NE6 TDCs containing shRNA were harvested and allophycocyanin was added and analyzed by flow cytometry (top). Proliferation was measured by BrdUrd incorporation (bottom). D, 76NE6 TDCs with ACLY downregulation were plated on a transwell chamber containing Matrigel and incubated on top of fibronectin-containing media for 24 hours. Invaded cells were stained with crystal violet. Images of ×20 magnification were taken with a light microscope. G, cells on the bottom of the transwell were collected at 24 hours and counted. Statistical analysis was conducted using the Student *t* test from three independent replicates. Error bars, SEM; *, $P < 0.05$ and **, $P < 0.005$.

the cell-cycle profiles or doubling times following ACLY downregulation (Supplementary Fig. S2C and S2D; Supplementary Table S3). The transwell invasion assay revealed that ACLY is required for LMW-E TDC-mediated invasion. LMW-E (T1) and LMW-E TDCs are inherently more invasive as can be seen by the increased number of invasive cells in the scrambled shRNA conditions compared with the parental and EL cells. However, invasive capacity of LMW-E TDCs was reduced up to 60% when ACLY was downregulated, with minimal or no effect in parental or EL cells (Fig. 5D and E). Levels of EMT-related genes such as E-cadherin, Twist, Slug, and Zeb1 were not altered by ACLY downregulation (Supplementary Fig. S3). Together, these data suggest that ACLY is required for migration and invasion of LMW-E TDCs and that cell cycle, proliferation, and EMT are unaffected.

ACLY is required for LMW-E–mediated tumor growth *in vivo*

To further examine the requirement of ACLY in LMW-E–mediated tumorigenesis, we performed an *in vivo* xenograft tumor assay and injected MCF7 cells containing both stable expression of the cyclin E isoforms and stable knockdown of ACLY into the mammary fat pad of nude mice. ACLY downregulation in vector-expressing cells modestly reduced tumor growth, compared with EL-expressing tumors with ACLY knockdown (Fig. 6A and B and Supplementary Fig. S4A). However, ACLY downregulation in LMW-E–expressing cells substantially inhibited tumor growth (Fig. 6A and B). Specifically, tumor volumes from vector-expressing cells increased 3-fold and tumor volumes from EL-expressing cells increased 6-fold. LMW-E–expressing cells containing ACLY downregulation exhibited virtually no change in tumor volume over the 10-week period (Fig. 6A). These changes were corroborated with examination of tumor weight. Specifically, LMW-E–expressing tumors with ACLY downregulation were extremely small with weights ranging from 6 to 65 mg, whereas vector and EL-expressing tumors displayed weights ranging from 200 to 400 mg (Supplementary Fig. S4B). We also observed ACLY knockdown in LMW-E–expressing tumors delays tumor latency. Specifically, shACLY transcript #1 delayed tumor formation by 6 weeks in LMW-E (T1) and up to 9 weeks in LMW-E (T2)–expressing tumors. Similarly, tumor formation was delayed in cells expressing shACLY transcript #2, with tumors only forming in 40% of mice after 12 weeks (Supplementary Table S4). Hematoxylin and eosin (H&E) staining revealed moderate to poorly differentiated invasive ductal carcinoma with desmoplastic stroma in all tumor samples (Fig. 6C). We confirmed reduced expression of ACLY in knockdown ACLY tumors. Cyclin E expression was localized to the nucleus in EL-expressing tumors, whereas LMW-E–expressing tumors displayed cyclin E localization to the nucleus and cytoplasm (Fig. 6C; Supplementary Table S5). ACLY knockdown also increased Ki67 positivity for only vector and EL-expressing tumors (Fig. 6C and Supplementary Fig. S4C; Supplementary Table S5). To interrogate the ability of LMW-E expression to induce lipid production, we stained the mouse tumors with Oil Red O (Fig. 6D). Vector- and EL-expressing tumors showed no lipid accumulation whereas LMW-E–expressing tumors displayed neutral lipid accumulation that was reversed upon ACLY downregulation (Fig. 6D). Using tumor xenografts, we also show that acetyl-CoA levels remain unchanged in vector- or EL-expressing cells containing ACLY knockdown, whereas acetyl-CoA in LMW-E–expressing cells containing ACLY knockdown increases significantly compared with controls (Supplementary Fig. S4D). In addition, oxaloacetate and citrate levels in these conditions remain unchanged overall (Supplementary Fig. S4D).

These results suggest that substrates that are upstream of ACLY, especially acetyl-CoA in the TCA cycle, accumulate intracellularly, due to lack of the ACLY enzyme downstream in the *de novo* lipogenesis pathway. We also measured *de novo* synthesis of lipids in the MCF-7 panel of cell lines and the results reveal that although MCF-7-EL cells require glucose-derived lipid biosynthesis for their tumorigenic potential that MCF-7-LMW-E cells are not dependent on this process (Supplementary Fig. S4D).

These results prompted us to interrogate if other markers of lipid biogenesis are also modulated by LMW-E expression and ACLY downregulation. One such marker is adipophilin, a major protein on the surface of lipid droplets. We examined expression of adipophilin in mouse tumor xenografts and results revealed that high adipophilin levels correlate with LMW-E and ACLY expression, but adipophilin levels decrease significantly upon ACLY downregulation (Fig. 6C; Supplementary Table S5). Taken together, these results show that LMW-E tumors require ACLY-mediated lipid-based energy or building blocks for efficient tumor formation and growth.

Adipohilin levels correlate with LMW-E and poor prognosis in breast cancer patients

RePCA analysis revealed that LMW-E interacts with ACLY in the cytoplasm and upregulates ACLY enzymatic activity, leading to lipid droplet formation. Therefore, we examined the concordance of LMW-E expression and lipid accumulation in tumor tissue from 100 breast cancer patients. Clinical and pathologic variables are summarized in Supplementary Table S1. Recently, antibodies that recognize proteins associated with lipid droplets, such as adipophilin, have been described using paraffin sections in various cancer types, including breast cancer (Supplementary Fig. S5; Supplementary Table S6; refs. 45, 46). Here we used adipophilin IHC to determine the intracytoplasmic lipid accumulation in breast carcinoma samples. A strong correlation was observed between cytoplasmic cyclin E staining and adipophilin staining ($P = 0.0001$; Fig. 7A and B). Specifically, 100% of patient samples negative for LMW-E expression also had negative/low adipophilin expression, whereas 40% of all patients containing LMW-E expression also had high adipophilin expression. Next, we set out to investigate the correlation of cyclin E and adipophilin expression in different subtypes of breast cancer. We observed significant differences in the distribution of breast cancer subtypes between tumors harboring and lacking adipophilin (Fig. 7C) and cyclin E (Fig. 7D). Overall, luminal A-like ($ER^+/PR^+/Ki67^{low}$) and luminal B ($ER^+/PR^+/Ki67^{high}$) subtype breast tumors were significantly less likely to have LMW-E and adipophilin expression compared with HER2-positive and TNBC subtypes. Finally, we investigated the clinical significance of adipophilin and/or LMW-E expression in our patient cohort. Kaplan–Meier recurrence-free survival curves as a function of adipophilin, cyclin E, and the combination of cyclin E and adipophilin staining are shown in Fig. 7E–G, respectively. Lack of LMW-E and low adipophilin scores were associated with a favorable prognosis, whereas overexpression of both proteins was correlated with a significantly worse prognosis.

Discussion

In this study, we identified ACLY as a novel binding partner of cyclin E and demonstrated that this interaction contributes to the aggressiveness of breast cancer by enhancing ACLY function. Although all isoforms of cyclin E bind ACLY, it is only cytoplasmic

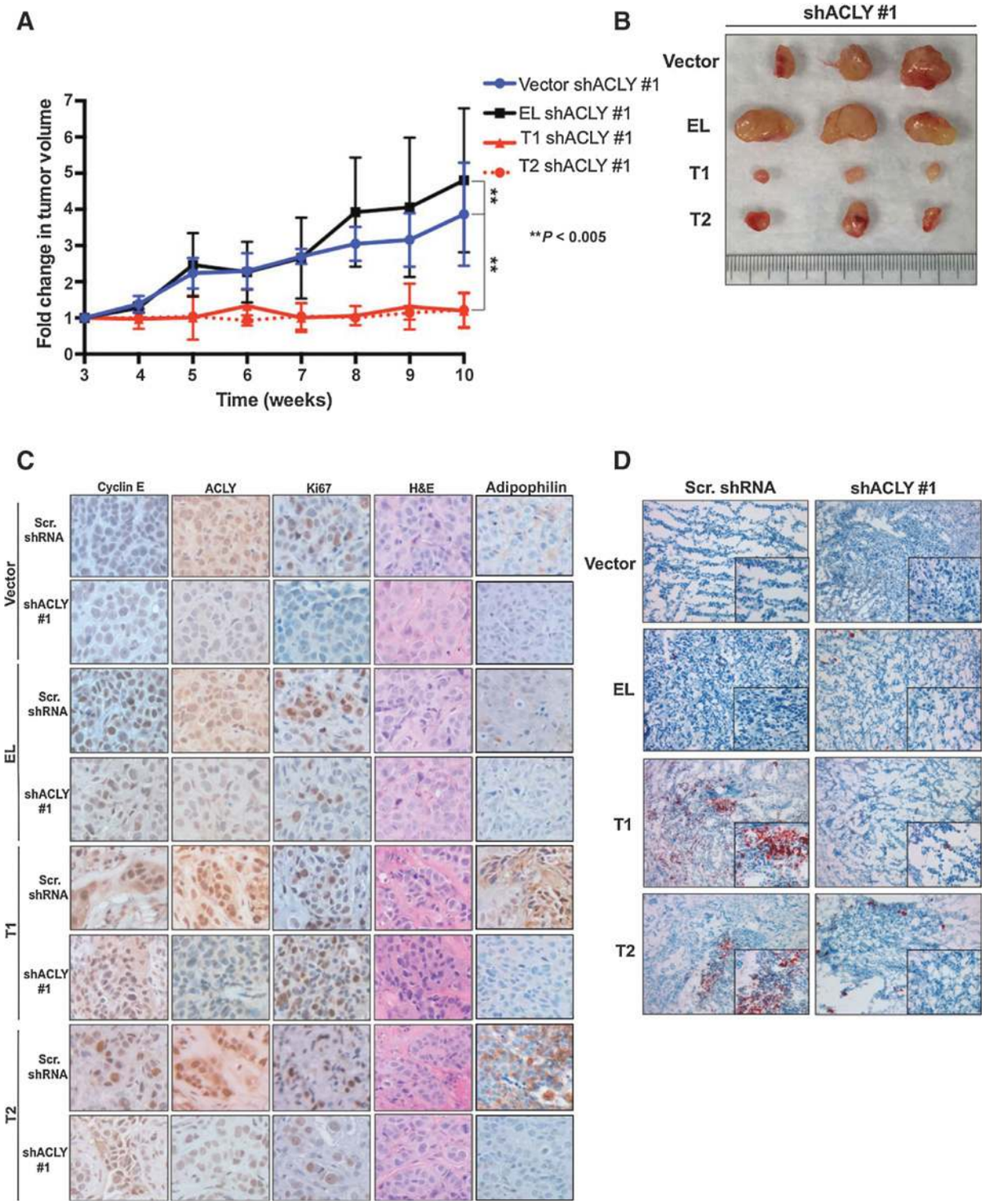

Figure 6.

ACLY is required for LMW-E–mediated tumor growth. A, inhibition of tumor growth in MCF7 cells containing stable overexpression of the cyclin E isoforms and either scrambled shRNA or shRNA targeted to ACLY. Tumors were measured for 10 weeks starting at 3 weeks. Statistical analysis was conducted using the Student *t* test. $N = 5$; error bars, SEM; **, $P < 0.005$. B, representative picture of shACLY#1 tumors. C, representative sections from tumors expressing the cyclin E isoforms were examined for the expression of cyclin E, ACLY, Ki-67, and adipophilin antibodies by immunohistochemical staining. H&E staining revealed the morphology of the tumor. Images are at ×20 magnification. D, neutral lipid accumulation in tissues from tumor xenografts. Magnification is ×10 per group. Insets from the images are magnified ×40 to highlight the lipid-staining morphology.

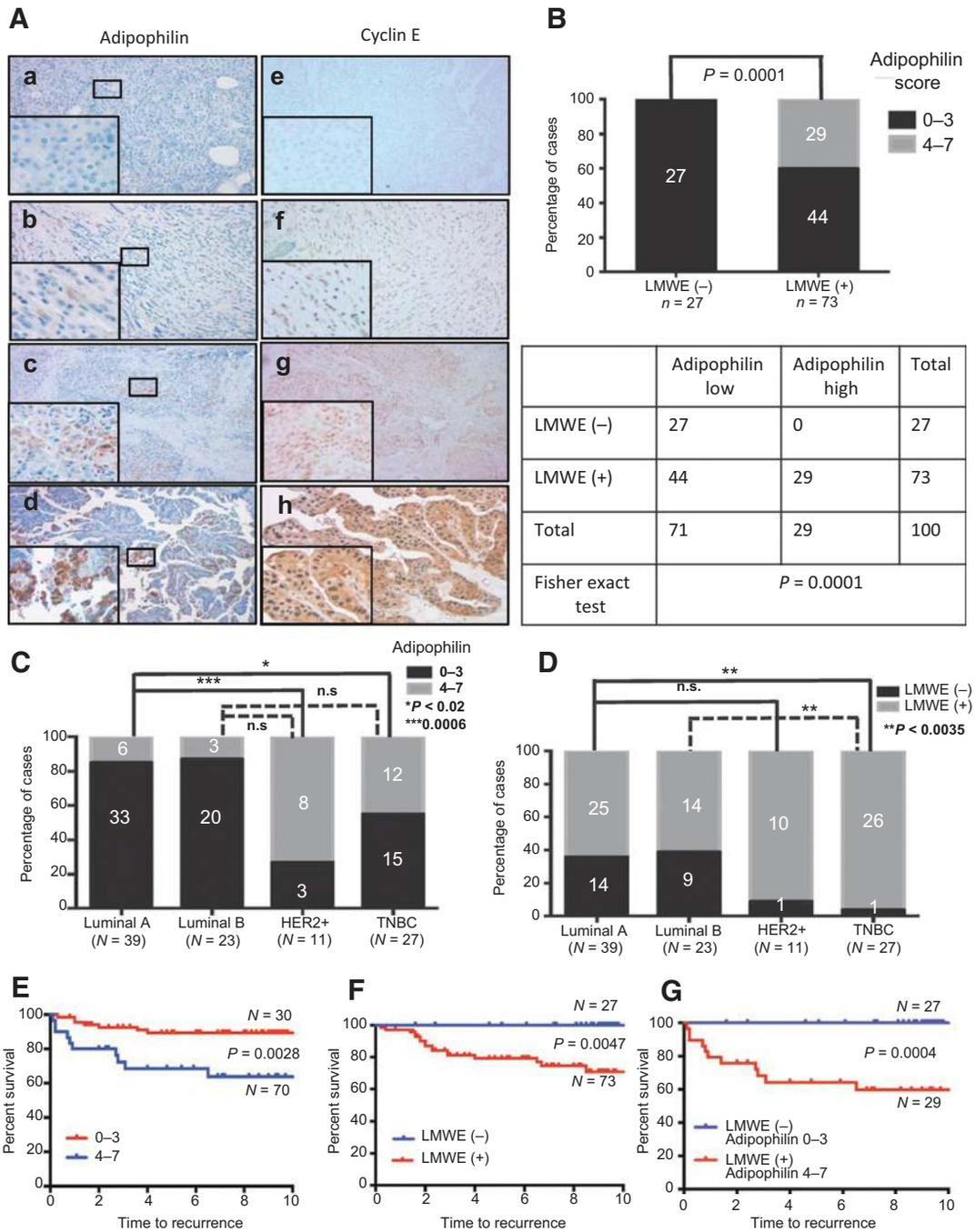

	Adipophilin low	Adipophilin high	Total
LMWE (–)	27	0	27
LMWE (+)	44	29	73
Total	71	29	100
Fisher exact test	*P* = 0.0001		

Figure 7.
Analysis of LMWE and/or adipophilin expression in breast cancer patients. A, representative images of immunohistochemical staining for adipophilin and correlation with expression of cyclin E are shown (magnification, ×100; magnification of inset images, ×400). Specifically, adipophilin (a and b) and corresponding cyclin E (e and f) staining for low adipophilin/LMWE (−); adipophilin (c and d) and corresponding (g and h) for high adipophilin/LMWE (+) expression. B, association between adipophilin and cyclin E expression in 100 invasive breast carcinoma tissue specimens, determined using Fisher exact test. The results revealed that there was a significantly positive correlation between the expression levels of adipophilin and cytoplasmic cyclin E (LMW-E +) expression ($P < 0.001$). Corresponding table shows significant positive correlation of staining of adipophilin and cytoplasmic cyclin E expression in the 100 human breast tumor samples examined. Quantification of adipophilin (C) and cyclin E (D) expression in the different subtypes of invasive breast carcinoma tissue specimens. Frequency distribution illustrating the percentage of cases, evaluated by IHC, falling into each categorical score over the range 0 to 7 (see Supplementary Table S5) for luminal A, luminal B, HER-2 (+), and triple-negative breast carcinoma (TNBC); statistical significance determined by Fisher exact test. n.s., not significant. E and F, Kaplan–Meier survival plots demonstrating the association between adipophilin and LMWE expression and breast cancer recurrence-free survival in 100 invasive breast carcinoma patients. G, Kaplan–Meier survival plots demonstrating the association between combined adipophilin and cyclin E expression and breast cancer recurrence-free survival in 100 invasive breast carcinoma patients.

LMW-E that affects ACLY function. Full-length cyclin E (EL) is primarily localized to the nucleus, whereas LMW-Es are predominately cytoplasmic (23). Enzymatic activation of ACLY occurs only by cytoplasmic LMW-E and it is possible that LMW-E binding induces a conformational change in ACLY and creates a stronger binding pocket for citrate and ATP, thereby enhancing its enzymatic activity.

ACLY and other enzymes in the *de novo* lipogenesis pathway, such as acetyl-CoA carboxylase (ACC) and fatty acid synthase (FASN), have been shown to be upregulated in cancer cells and energy deregulation now recognized as an emerging hallmark of cancer and a characteristic of the transformed phenotype (43). We found that LMW-E expression results in lipid droplet formation. Lipid droplets (LD) provide intracellular energy and are composed of triacylglycerides and cholesteryl esters surrounded by a phospholipid monolayer (47). LDs and increased fatty acid synthesis have shown to be involved in many areas of cancer progression (47). In general, fatty acids not only promote membrane synthesis, which is required for cell growth and proliferation, but also exhibit nonproliferative roles. For example, fatty acids lead to membrane fluidity important for resistance to oxidative stress and survival under energy stress (47). Moreover, metabolic intermediates such as NADPH provide redox balance and fatty acid–derived lipids facilitate signaling through membrane receptors or lipid-based posttranslational modifications (47).

Although it is counterintuitive for breast cancer cells to upregulate lipid production due to residing in a lipid-rich environment, other groups have shown similar results. Activation of *de novo* lipid synthesis in cancer cells has shown to be irrespective of environment; *in vivo* labeling using ^{14}C-glucose determined that most esterified fatty acids derived in tumor models were derived from *de novo* lipid synthesis (48). Furthermore, 93% of triacylglycerol fatty acids in tumor cells are derived from *de novo* synthesis (43). In breast cancer, human growth hormone stimulation increases lipid synthesis and forms cytoplasmic lipid droplets in T47D luminal breast cancer cells (49) and the lipid phenotype can easily stratify malignancy in breast cancer (50). These observations are consistent with our findings that genetic downregulation of ACLY resulted in reduced anchorage-independent growth *in vitro* and xenograft tumor growth *in vivo* that was specific to LMW-E–expressing breast cancer cells. In tumor xenografts, LMW-E expression concomitantly with ACLY downregulation significantly increases acetyl-CoA levels compared with controls. These results suggest that substrates upstream of ACLY, especially acetyl-CoA in the TCA cycle, accumulate intracellulary, due to lack of the ACLY enzyme downstream in the *de novo* lipogenesis pathway. These results also imply that the binding and interaction between ACLY and LMW-E may be a rate limiting step in the *de novo* lipogenesis pathway and when one element is removed (i.e., ACLY) the lipogenesis pathway is inhibited despite multiple compensatory pathways for acetyl-CoA production.

Finally, we interrogated whether other markers of lipid biogenesis are also modulated by LMW-E expression and if these levels are altered by ACLY downregulation. We found that adipophilin levels are high in tumor xenografts and breast cancer patient samples with LMW-E and ACLY and that adipophilin levels decrease significantly when ACLY is downregulated. Moreover, this flux is absent when EL is expressed. In patient samples, coexpression of adipophilin and LMW-E lead to decreased survival and poor prognosis, whereas those patients with low adipophilin and no LMW-E expression had 100% progression-free survival. Therefore, inhibition of ACLY and reduction of lipid accumulation may prove to be beneficial in targeting other aggressive cancer types that display LMW-E expression such as ovarian, colorectal cancers, and melanoma.

Disclosure of Potential Conflicts of Interest

G.B. Mills reports receiving commercial research grants from Adelson Medical Research Foundation, AstraZeneca, Critical Outcome Technology, Komen Research Foundation, and Nanostring; has received speakers' bureau honoraria from AstraZeneca, ISIS Pharmaceuticals, Nuevolution, and Symphogen; has ownership interest (including patents) in Catena Pharmaceuticals, Myriad Genetics, PIV Ventures, and Spindletop Ventures; and is a consultant/advisory board member for Adventist Health, AstraZeneca, Blend, Catena Pharmaceuticals, Critical Outcome Technologies, HanAl Bio Korea, ImmunoMET, Millenium Pharmaceuticals, Nuevolution, Precision Medicine Provista Diagnostics, Signalchem Lifesciences, and Symphogen. No potential conflicts of interest were disclosed by the other authors.

Authors' Contributions

Conception and design: K.S. Lucenay, G.B. Mills, K.K. Hunt, K. Keyomarsi
Development of methodology: K.S. Lucenay, I. Doostan, Z. Ding, K. Keyomarsi
Acquisition of data (provided animals, acquired and managed patients, provided facilities, etc.): K.S. Lucenay, I. Doostan, C. Karakas, G.B. Mills, K.K. Hunt, K. Keyomarsi
Analysis and interpretation of data (e.g., statistical analysis, biostatistics, computational analysis): K.S. Lucenay, C. Karakas, G.B. Mills, K.K. Hunt, K. Keyomarsi
Writing, review, and/or revision of the manuscript: K.S. Lucenay, G.B. Mills, K. Keyomarsi
Administrative, technical, or material support (i.e., reporting or organizing data, constructing databases): T. Bui, K. Keyomarsi
Study supervision: K.K. Hunt, K. Keyomarsi

Acknowledgments

This research was supported by NIH grants CA87458 and CA1522228 to K. Keyomarsi; by CPRIT training grant RP140106 (I. Doostan); by Komen SAC grant SAC110052 04, Komen Promise grant KG08169404, P01CA0099031 (G.B. Mills), and by CCSG grant P30 CA016672 to MD Anderson Cancer Center.

The costs of publication of this article were defrayed in part by the payment of page charges. This article must therefore be hereby marked *advertisement* in accordance with 18 U.S.C. Section 1734 solely to indicate this fact.

Received June 19, 2015; revised February 10, 2016; accepted February 16, 2016; published OnlineFirst February 29, 2016.

References

1. Mussman JG, Horn HF, Carroll PE, Okuda M, Tarapore P, Donehower LA, et al. Synergistic induction of centrosome hyperamplification by loss of p53 and cyclin E overexpression. Oncogene 2000;19:1635–46.
2. Keyomarsi K, Tucker SL, Buchholz TA, Callister M, Ding Y, Hortobagyi GN, et al. Cyclin E and survival in patients with breast cancer. N Engl J Med 2002;347:1566–75.
3. Porter DC, Zhang N, Danes C, McGahren MJ, Harwell RM, Faruki S, et al. Tumor-specific proteolytic processing of cyclin E generates hyperactive lower-molecular-weight forms. Mol Cell Biol 2001;21:6254–69.
4. Mombelli S, Cochaud S, Merrouche Y, Garbar C, Antonicelli F, Laprevotte E, et al. IL-17A and its homologs IL-25/IL-17E recruit the c-RAF/S6 kinase pathway and the generation of pro-oncogenic LMW-E in breast cancer cells. Sci Rep 2015;5:11874.
5. Tokai Y, Maeda S, Yamaguchi J, Uga T, Hayashida N, Taniguchi K, et al. Cyclin E low-molecular-weight isoform as a predictor of breast cancer in Japanese women. Int Surg 2011;96:245–53.
6. Taneja P, Maglic D, Kai F, Zhu S, Kendig RD, Fry EA, et al. Classical and novel prognostic markers for breast cancer and their clinical significance. Clin Med Insights Oncol 2010;4:15–34.

7. Rath SL, Senapati S. Why are the truncated cyclin Es more effective CDK2 activators than the full-length isoforms? Biochemistry 2014;53: 4612–24.
8. Loeb KR, Chen X. Too much cleavage of cyclin E promotes breast tumorigenesis. PLoS Genet 2012;8:e1002623.
9. Moore JD. In the wrong place at the wrong time: does cyclin mislocalization drive oncogenic transformation? Nat Rev Cancer 2013;13:201–8.
10. Bedrosian I, Lu KH, Verschraegen C, Keyomarsi K. Cyclin E deregulation alters the biologic properties of ovarian cancer cells. Oncogene 2004;23: 2648–57.
11. Davidson B, Skrede M, Silins I, Shih Ie M, Trope CG, Florenes VA. Low-molecular weight forms of cyclin E differentiate ovarian carcinoma from cells of mesothelial origin and are associated with poor survival in ovarian carcinoma. Cancer 2007;110:1264–71.
12. Bales E, Mills L, Milam N, McGahren-Murray M, Bandyopadhyay D, Chen D, et al. The low molecular weight cyclin E isoforms augment angiogenesis and metastasis of human melanoma cells *in vivo*. Cancer Res 2005;65: 692–7.
13. Corin I, Di Giacomo MC, Lastella P, Bagnulo R, Guanti G, Simone C. Tumor-specific hyperactive low-molecular-weight cyclin E isoforms detection and characterization in non-metastatic colorectal tumors. Cancer Biol Ther 2006;5:198–203.
14. Milne AN, Carvalho R, Jansen M, Kranenbarg EK, van de Velde CJ, Morsink FM, et al. Cyclin E low molecular weight isoforms occur commonly in early-onset gastric cancer and independently predict survival. J Clin Pathol 2008;61:311–6.
15. Corin I, Larsson L, Bergstrom J, Gustavsson B, Derwinger K. A study of the expression of Cyclin E and its isoforms in tumor and adjacent mucosa, correlated to patient outcome in early colon cancer. Acta Oncol 2010; 49:63–9.
16. Zhou YJ, Xie YT, Gu J, Yan L, Guan GX, Liu X. Overexpression of cyclin E isoforms correlates with poor prognosis in rectal cancer. Eur J Surg Oncol 2011;37:1078–84.
17. Koutsami MK, Tsantoulis PK, Kouloukoussa M, Apostolopoulou K, Pateras IS, Spartinou Z, et al. Centrosome abnormalities are frequently observed in non-small-cell lung cancer and are associated with aneuploidy and cyclin E overexpression. J Pathol 2006;209:512–21.
18. Nauman A, Turowska O, Poplawski P, Master A, Tanski Z, Puzianowska-Kuznicka M. Elevated cyclin E level in human clear cell renal cell carcinoma: possible causes and consequences. Acta Biochim Pol 2007;54:595–602.
19. Akli S, Van Pelt CS, Bui T, Multani AS, Chang S, Johnson D, et al. Overexpression of the low molecular weight cyclin E in transgenic mice induces metastatic mammary carcinomas through the disruption of the ARF-p53 pathway. Cancer Res 2007;67:7212–22.
20. Akli S, Zheng PJ, Multani AS, Wingate HF, Pathak S, Zhang N, et al. Tumor-specific low molecular weight forms of cyclin E induce genomic instability and resistance to p21, p27, and antiestrogens in breast cancer. Cancer Res 2004;64:3198–208.
21. Wingate H, Zhang N, McGarhen MJ, Bedrosian I, Harper JW, Keyomarsi K. The tumor-specific hyperactive forms of cyclin E are resistant to inhibition by p21 and p27. J Biol Chem 2005;280:15148–57.
22. Moore JD, Yang J, Truant R, Kornbluth S. Nuclear import of cdk/cyclin complexes: Identification of distinct mechanisms for import of cdk2/cyclin E and cdc2/cyclin B1. J Cell Bio 1999;144:213–24.
23. Delk NA, Hunt KK, Keyomarsi K. Altered subcellular localization of tumor-specific cyclin E isoforms affects cyclin-dependent kinase 2 complex formation and proteasomal regulation. Cancer Res 2009;69: 2817–25.
24. Ding Z, Liang J, Lu Y, Yu Q, Songyang Z, Lin SY, et al. A retrovirus-based protein complementation assay screen reveals functional AKT1-binding partners. Proc Natl Acad Sci U S A 2006;103:15014–9.
25. Nanos-Webb A, Jabbour NA, Multani AS, Wingate H, Oumata N, Galons H, et al. Targeting low molecular weight cyclin E (LMW-E) in breast cancer. Breast Cancer Res Treat 2012;132:575–88.
26. Duong MT, Akli S, Wei C, Wingate HF, Liu W, Lu Y, et al. LMW-E/CDK2 deregulates acinar morphogenesis, induces tumorigenesis, and associates with the activated b-Raf-ERK1/2-mTOR pathway in breast cancer patients. PLoS Genet 2012;8:e1002538.
27. Duong MT, Akli S, Macalou S, Biernacka A, Debeb BG, Yi M, et al. Hbo1 is a cyclin E/CDK2 substrate that enriches breast cancer stem-like cells. Cancer Res 2013;73:5556–68.
28. Migita T, Narita T, Nomura K, Miyagi E, Inazuka F, Matsuura M, et al. ATP citrate lyase: activation and therapeutic implications in non-small cell lung cancer. Cancer Res 2008;68:8547–54.
29. Hatzivassiliou G, Zhao F, Bauer DE, Andreadis C, Shaw AN, Dhanak D, et al. ATP citrate lyase inhibition can suppress tumor cell growth. Cancer Cell 2005;8:311–21.
30. Bauer DE, Hatzivassiliou G, Zhao F, Andreadis C, Thompson CB. ATP citrate lyase is an important component of cell growth and transformation. Oncogene 2005;24:6314–22.
31. Morrison DK. The 14-3-3 proteins: integrators of diverse signaling cues that impact cell fate and cancer development. Trends Cell Biol 2009;19:16–23.
32. Jego G, Hazoume A, Seigneuric R, Garrido C. Targeting heat shock proteins in cancer. Cancer Lett 2013;332:275–85.
33. Wong SH, Zhang T, Xu Y, Subramaniam VN, Griffiths G, Hong W. Endobrevin, a novel synaptobrevin/VAMP-like protein preferentially associated with the early endosome. Mol Biol Cell 1998;9:1549–63.
34. Hayashi N, Yokoyama N, Seki T, Azuma Y, Ohba T, Nishimoto T. RanBP1, a Ras-like nuclear G protein binding to Ran/TC4, inhibits RCC1 via Ran/TC4. Mol Gen Genet 1995;247:661–9.
35. Moon YA, Horton JD. Identification of two mammalian reductases involved in the two-carbon fatty acyl elongation cascade. J Biol Chem 2003;278:7335–43.
36. Szutowicz A, Kwiatkowski J, Angielski S. Lipogenetic and glycolytic enzyme activities in carcinoma and nonmalignant diseases of the human breast. Br J Cancer 1979;39:681–7.
37. Chypre M, Zaidi N, Smans K. ATP-citrate lyase: a mini-review. Biochem Biophys Res Commun 2012;422:1–4.
38. Beckner ME, Fellows-Mayle W, Zhang Z, Agostino NR, Kant JA, Day BW, et al. Identification of ATP citrate lyase as a positive regulator of glycolytic function in glioblastomas. Int J Cancer 2010;126:2282–95.
39. Berwick DC, Hers I, Heesom KJ, Moule SK, Tavare JM. The identification of ATP-citrate lyase as a protein kinase B (Akt) substrate in primary adipocytes. J Biol Chem 2002;277:33895–900.
40. Potapova IA, El-Maghrabi MR, Doronin SV, Benjamin WB. Phosphorylation of recombinant human ATP:citrate lyase by cAMP-dependent protein kinase abolishes homotropic allosteric regulation of the enzyme by citrate and increases the enzyme activity. Allosteric activation of ATP:citrate lyase by phosphorylated sugars. Biochemistry 2000;39:1169–79.
41. Wagner PD, Vu ND. Phosphorylation of ATP-citrate lyase by nucleoside diphosphate kinase. J Biol Chem 1995;270:21758–64.
42. Wellen KE, Hatzivassiliou G, Sachdeva UM, Bui TV, Cross JR, Thompson CB. ATP-citrate lyase links cellular metabolism to histone acetylation. Science 2009;324:1076–80.
43. Menendez JA, Lupu R. Fatty acid synthase and the lipogenic phenotype in cancer pathogenesis. Nat Rev Cancer 2007;7:763–77.
44. Walther TC, Farese RV Jr. Lipid droplets and cellular lipid metabolism. Annu Rev Biochem 2012;81:687–714.
45. Ostler DA, Prieto VG, Reed JA, Deavers MT, Lazar AJ, Ivan D. Adipophilin expression in sebaceous tumors and other cutaneous lesions with clear cell histology: an immunohistochemical study of 117 cases. Mod Pathol 2010; 23:567–73.
46. Straub BK, Herpel E, Singer S, Zimbelmann R, Breuhahn K, Macher-Goeppinger S, et al. Lipid droplet-associated PAT-proteins show frequent and differential expression in neoplastic steatogenesis. Mod Pathol 2010; 23:480–92.
47. Santos CR, Schulze A. Lipid metabolism in cancer. FEBS J 2012;279: 2610–23.
48. Medes G, Thomas A, Weinhouse S. Metabolism of neoplastic tissue. IV. A study of lipid synthesis in neoplastic tissue slices *in vitro*. Cancer Res 1953; 13:27–9.
49. Shiu RP, Paterson JA. Alteration of cell shape, adhesion, and lipid accumulation in human breast cancer cells (T-47D) by human prolactin and growth hormone. Cancer Res 1984;44:1178–86.
50. Nieva C, Marro M, Santana-Codina N, Rao S, Petrov D, Sierra A. The lipid phenotype of breast cancer cells characterized by Raman microspectroscopy: towards a stratification of malignancy. PLoS One 2012;7:e46456.